

The rise of Single-Atom Catalysts

Deepak Kumar Rai *

*Department of Chemistry, Southern University of Science and Technology, Shenzhen
518000, China*

E-mail: dkriitb@gmail.com

Abstract

In recent years, single-atom catalysts attracted lots of attention because of their high catalytic activity, selectivity, stability, maximum atom utilization, exceptional performance, and low cost. Single-atom catalyst contains isolated individual atom which are coordinated with the surface atoms of support such as a metal oxide or 2d - materials. In this review article, we present the advancement in single-atom catalysis in recent years with a focus on the various synthesis methods and their application in catalytic reactions. We also demonstrate the reaction mechanism of a single-atom catalyst for different catalytic reactions from theoretical aspects using density functional theory.

Introduction

In today's modern society, catalysts are widely used in the industrial sectors such as petroleum refining, fuel cells, chemical intermediates, pharmaceuticals, reduction of emission, and agrochemicals to increase the reaction rate of the desired chemical reaction¹⁻⁷. The conventional supported heterogeneous catalysts contain clusters or nanoparticles dispersed on the surfaces of appropriate support (i.e., metal oxides, 2d-materials, or porous metal-organic frameworks nanomaterials). The atom utilization and selectivity of conventional heterogeneous catalysts are very less, as only a part with a suitable size of clusters or nanoparticles participates in the catalytic reaction. Moreover, the remaining portion of clusters or nanoparticles does not participate in the catalytic reaction, and it is not useful, may be involved in unwanted reactions. The heterogeneous catalysts involved in petroleum refining, new energy application, emission reduction, and pharmaceuticals contain noble metal atoms like Pt, Pd, Ru, Rh, Ir, Ag, and Au. These noble metals are costly and low abundant in nature because of that these catalyst does not meet the current increasing demand of industries, resulting minimization of the use of such catalyst alter the catalytic activity of chemical reaction^{8,9}. To overcome

these issues, researchers have found the most promising way to increase the atom utilization and selectivity of catalysts by reducing the size of nanoclusters to isolated individual atoms, resulting in a catalyst containing a single atom on the surface of a support.

Single-atom catalysts (SACs) is a new class of catalyst which contain isolated individual isolated atom dispersed or coordinated with the surface atom of support. It exhibits high catalytic activity, stability, selectivity, and 100 % atom utilization because the whole surface area of a single atom is exposed to reactants in catalytic reactions^{10–15}. In 2011, Zhang and co-workers¹⁶ were the first to synthesized and investigate experimentally and theoretically the catalytic activity, selectivity and stability of single-atom Pt₁/FeO_x catalyst for CO oxidation. After that, It has attracted a lot of researchers, and numerous SACs have been synthesized and developed in recent years. By combining different noble atoms with different supports such as metal oxides, 2d-materials, or porous metal-organic frameworks (MOFs) nanomaterials. The SACs fabricated on different supports such as on metal oxides, 2d-materials, MOFs are [Pt₁/FeO_x¹⁶, Rh/ZrO₂¹⁷, Pt/ θ -Al₂O₃¹⁸, Ir₁/FeO_x¹⁹, Au₁/CeO₂²⁰, Au₁/Co₃O₄²¹, Au₁/FeO_x²², Pd/FeO_x²³, Pd₁/TiO₂²⁴], [Pt/g-C₃N₄²⁵, Pt/MoS₂²⁶, Pt/GNS²⁷, Pd₁/graphene²⁸], [Co-SAs/N-C²⁹, Fe-SAs/N-C³⁰, Ni-SAs/N-C³¹, and Ru-SAs/N-C³²], respectively. It has emerged as a new frontier in catalysis science because of its excellent performance.

In recent years, many researchers have reported that SACs shows excellent performance in various catalytic reactions, such as CO oxidation^{16,18,22,33–36}, water–gas shift (WGS)^{19,37–42}, water splitting, hydrogenation reaction, carbon dioxide reduction, etc. Despite the excellent performance of SACs, it has some limitations and disadvantages. The stabilization of single atoms on the surfaces of support is a very challenging process due to the agglomeration of single-atoms. It needs advanced techniques for synthesis, which we have discussed in the next section.

Remainder of the paper is organized as follows. In the next section II, we briefly discuss the advanced synthesis methods of SACs, while in section III, we describe the application of

SACs for different chemical reactions and their reaction mechanism from theoretical aspects. Finally in section IV, we summarize our review article.

Synthesis of Single Atom Catalysis

In this section, we present the various synthesis methods for the fabrication of single-atom catalysts. The stabilization of single atom on the surfaces of metal oxide or two-dimensional materials is a very challenging process due to the agglomeration of single-atoms and the tendency to form nanoparticles and clusters on the surfaces. The agglomeration of single atoms happens because the surface energy of nanoparticles and clusters is less than single-atom. So, advanced synthesis methods such as impregnation method, co-precipitation method, other-wet-chemical synthesis method, atomic layer deposition method, and metal-organic frameworks derived method are used for fabrication single-atom catalysts , are discussed below.

Impregnation Method

For the synthesis of the single-atom or supported catalyst impregnation method is the simplest and economical method. In this method, a small amount of solution containing active metal precursor is mixed with catalyst support, and using the ion-exchange and adsorption process active metals stabilized on the surface of support. Li et al.²⁵ synthesized Pt/g-C₃N₄ (see Fig. 1 A) by performing liquid phase reaction between graphitic carbon nitride (g-C₃N₄) and H₂PtCl₆, followed by annealing at low temperature, and this catalyst exhibit high activity for H₂ evolution. They prepared four samples of supported catalyst with different weight percentage (i.e. 0.075%, 0.11%, 0.16%, 0.38%) of metal loading, and found that at 0.16 wt% a bright spot center of Pt atoms are distributed on the surface on the surface of g-C₃N₄, can be seen in HAAD-STEM images. When the weight percentage is increased, up to 0.38% aggregation of small Pt atoms is observed on the surface. Yang et al.⁴³ prepared Pt/TiN

catalyst (see Fig. 1 B) using wetness impregnation method, in which a small amount (0.35 wt%) of Pt atoms is loaded on the surface of acid-treated TiN support, and this catalyst is found to be active for oxygen reduction reactions, formic acid, and methanol oxidation.

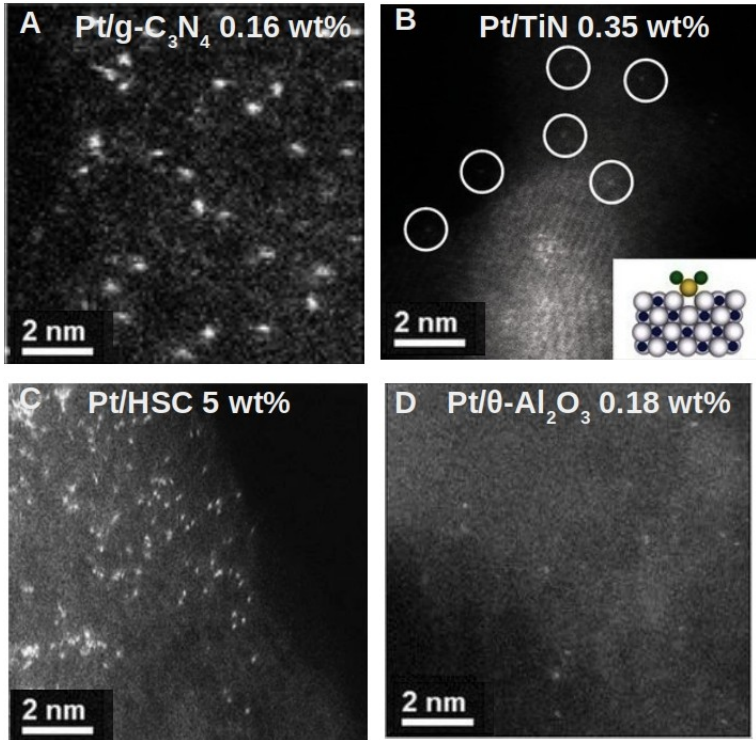


Figure 1: The figure represents the HAADF-STEM images of different single atom catalysts synthesized using impregnation method: (a) Pt/g-C₃N₄, (b) Pt/TiN, (c) Pt/LSC, (d) Pt/θ-Al₂O₃. (a) reprinted/reproduce from Ref. [25] with the permission of Wiley-VCH publishing group, copyright 2016, (b) reprinted/reproduce from Ref. [43] with the permission of Wiley-VCH publishing group, copyright 2016, (c) reprinted/reproduce from Ref. [44] with the permission of Nature publishing group, copyright 2016, (d) reprinted/reproduce from Ref. [18] with the permission of American Chemical society publishing group, copyright 2013.

Yang et al. observed the formation of Pt nanoparticles on the surface of support if the weight percentage is increased above 0.35%. Recently, Choi et al.⁴⁴ synthesized highly loaded (5 wt%) Pt/S-ZTC catalyst (see Fig. 1 C) using wet-impregnation method, in which Pt atom is atomically dispersed on the surface of sulfur-doped zeolite-templated carbon (S-ZTC). The doped sulfur and unique three-dimensional structure of ZTC stabilize the loaded Pt atoms on the support surface. They have reported Pt/S-ZTC exhibit high activity for

oxygen reduction reaction. Kwon et al.¹⁷ have studied the activation of methane for methanol production using Rh/ZrO₂SACs, which the prepared by wet impregnation method.

Moses-DeBusk et al.¹⁸ have studied the CO oxidation activity of a single Pt atom supported on θ -alumina (θ -Al₂O₃). They have synthesized Pt/ θ -Al₂O₃ SAC (see Fig. 1 D) by mixing alumina in an aqueous solution of chloroplatinic acid, heated at mild temperature for 30 hours, and placed on a rotovap for water evaporation. Resulting free flow powder is kept in an alumina crucible, and pyrolysis is done with elevated temperature 1 °C/min to 450 °C for 4 hours for obtaining Pt/ θ -Al₂O₃ SAC. The HAADF-STEM images of single atoms catalysts Pt/g-C₃N₄²⁵, Pt/TiN⁴³, Pt/LSC⁴⁴ and Pt/ θ -Al₂O₃¹⁸ with 0.16 wt%, 0.35 wt%, 5wt% and 0.18 wt%, respectively, are presented in Fig. 1.

It is challenging to produce uniformly distributed and highly loaded SACs with this method because it depends on the ability of support to adsorb the metal atoms, .i.e, the loading and distribution depends on the number of anchoring sites present on the surface of support.

Co-precipitation Method

Co-precipitation is a convenient, cost-effective, and less time-consuming method for the synthesis of nanoparticles. This method is slightly different from the impregnation method; here, metals atom are incorporated in the interstitial sites of support, not distributed on the surface of the support. In this method, anionic and cationic solution are mixed and simultaneously nucleation, growth, coarsening, and/or agglomeration processes starts. After agglomeration, we have to followed three more steps, i.e., precipitation, filtration, and calcination, and finally, nanoparticle is obtained. Recently, Zhang’s research group have reported that they were the first one to fabricate SAC containing isolated Pt atoms uniformly dispersed on the iron oxide (FeO_x) support using the co-precipitation method^{16,45}. Two samples of Pt₁/FeO_x (see Fig. 2 A) were prepared, with 0.17 wt% and 2.5 wt%, using an aqueous solution of chloroplatinic acid (H₂PtCl₆.6H₂O) and ferric nitrate Fe(NO₃)₃.9H₂O

with precipitation agent sodium carbonate (Na_2CO_3) at 50 °C, and the PH value is maintained around 8. The resulting sample was dried at 60 °C for five hours and calcined at 400 °C for five hours. Furthermore, samples were reduced at 200 °C for half an hour with 10% H_2/He flow rate. They also reported that at low Pt loading 0.17 wt%, uniformly dispersed isolated Pt atom on the FeO_x support can be seen HAADF images, whereas, at 2.5 wt%, mixture of Pt atoms, 2D structure of Pt atoms and cluster of Pt atoms is observed. This SAC shows excellent activity and stability for CO oxidation and NO reduction.

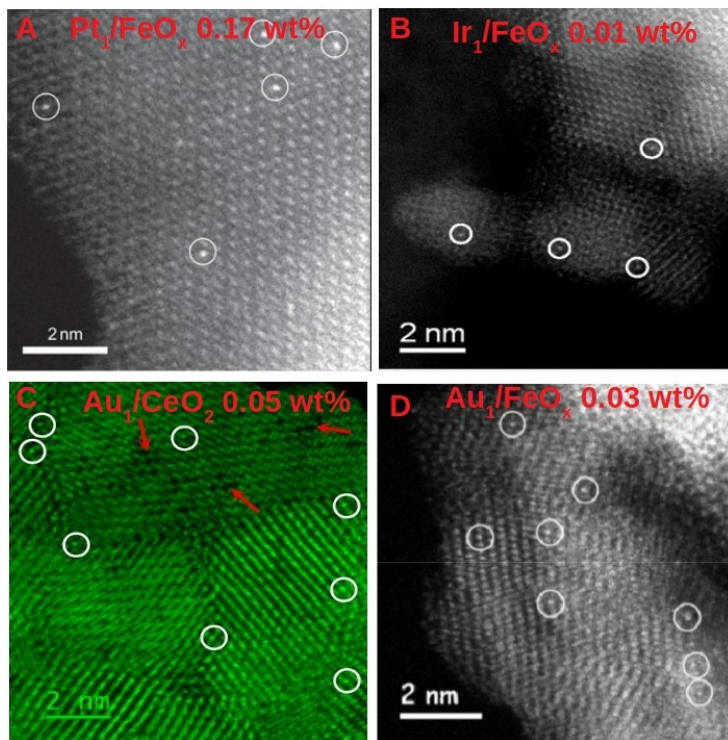


Figure 2: The figure represents the HAADF-STEM images of different single atom catalyst synthesized using co-precipitation method: (a) Pt_1/FeO_x , (b) Ir_1/FeO_x , (c) Au_1/CeO_2 , (d) Au_1/FeO_x . (a) reprinted/reproduce from Ref. [16] with the permission of Nature publishing group, copyright 2011, (b) reprinted/reproduce from Ref. [19] with the permission of American Chemical society publishing group, copyright 2013, (c) reprinted/reproduce from Ref. [20] with the permission of American Chemical society publishing group, copyright 2015, (d) reprinted/reproduce from Ref. [22] with the permission of Tsinghua university press and Springer publishing group, copyright 2015.

In addition to that Zhang and co-workers, using co-precipitation method, have synthesized series of SACs such as Ir_1/FeO_x ¹⁹ (see Fig. 2 B), Au_1/CeO_2 ²⁰ (see Fig. 2 C),

$\text{Au}_1/\text{Co}_3\text{O}_4$ ²¹, Au_1/FeO_x ²² (see Fig. 2 D), and Pd/FeO_x ²³, which exhibits excellent activity and stability for water-gas shift reactions and CO oxidation.

Xing et al.⁴⁶ have prepared single atom photo-catalyst containing isolated metal atoms (Pt, Pd, Ru and Rh) uniformly dispersed on titanium oxide (TiO_2) support using co-precipitation method and studied their activity and stability for water-splitting reaction. They have synthesized 4 samples for Pt/ TiO_2 with different metal loading percentage 0.2 wt%, 0.5 wt%, 2wt% and 1Pt/ TiO_2 (PD) (pure photo deposited 1 wt% of Pt nanoparticles), and found that H_2 evolution rate for 0.2-Pt/ TiO_2 is 169.6 $\mu\text{mol/h}$, which is 23, 57, and 136 times more than 1Pt/ TiO_2 (PD), 0.5-Pt/ TiO_2 and 2-Pt/ TiO_2 , respectively. The H_2 evolution rate for Pd, Ru, and Rh nanoparticles supported on TiO_2 is 7, 7 and 13 times less than 0.2-Pt/ TiO_2 , respectively. The HAADF-STEM images of single atoms catalysts Pt_1/FeO_x ¹⁶, Ir_1/FeO_x ¹⁹, Au_1/CeO_2 ²⁰, and Au_1/FeO_x ²² with 0.17 wt%, 0.01 wt%, 0.05 wt% and 0.03 wt%, respectively, are presented in Fig. 2.

The advantages to this method are; it is a simple, rapid, easy to control the particle size and composition of the final product, energy-efficient and does not need organic solvent. Moreover, disadvantages of this method are; it does not apply to uncharged species, trace of impurities also get precipitated, reproducibility problem and does not work well if the reactants have very different precipitation rate.

Other Wet-Chemical Synthesis Method

Impregnation and Co-precipitation are the traditional wet-chemical synthesis method, but Liu et al.²⁴ have used unique wet-chemical synthesis methods for the fabrication of single atom Pd_1/TiO_2 catalyst (see Fig. 3 A) with a high metal loading up to 1.5 wt%. They dispersed a solution of H_2PdCl_4 on the surface of TiO_2 support, the resulting mixture is exposed to UV rays for 10 min. After that, the irradiated sample is washed with water, and a single atom Pd_1/TiO_2 catalyst is obtained. From transmission electron microscopy (TEM) images and extended x-ray absorption fine structure (EXAFS) spectra, it is concluded that

the formation of Pd clusters or nanoparticles are not observed. This catalyst exhibits very high catalytic activity and stability for the hydrogenation of C=C and C=O.

Recently, Li et al.²⁶ synthesized single atom Pt/MoS₂ catalyst (see Fig. 3 B) by injecting solution of K₂PtCl₆ using syringe pump into the mixture of MoS₂ nanosheets, ethanol, and water. During the chemisorption process, Mo atoms are replaced by Pt atoms in MoS₂ nanosheets. Pt/MoS₂ catalysts with different Pt loading percentages 0.2, 1.0, 5.0, 7.5 are synthesized by changing the concentration of K₂PtCl₆, and EXAFS spectra of all these catalysts confirmed that only isolated Pt is present on the surface of MoS₂. Researchers also investigated its catalytic activity for the conversion of CO₂ into methanol without the formation of formic acid. The HAADF-STEM images of single atoms catalysts Pd₁/TiO₂²⁴, and Pt₁/MoS₂²⁶ with 1.5 wt%, and 0.2 wt%, respectively, are presented in Fig. 3.

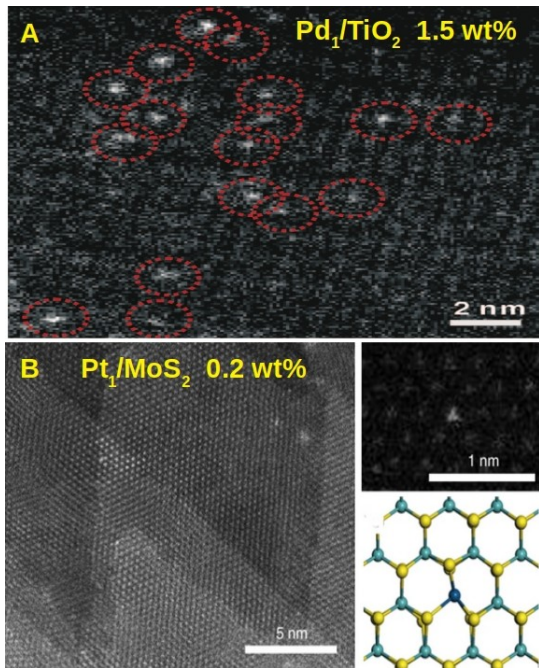


Figure 3: The figure represents the HAADF-STEM images of different single atom catalyst synthesized using other wet-chemical method: (a) Pd₁/TiO₂, (b) Pt₁/MoS₂. (a) reprinted/reproduce from Ref. [24] with the permission of Science publishing group, copyright 2016, (b) reprinted/reproduce from Ref. [26] with the permission of Macmillan Publishers Limited and part of Springer Nature publishing group, copyright 2018.

Atomic Layer Depositions Method

Atomic layer deposition (ALD) is a subclass of chemical vapor deposition, attracting many researchers because of its ability to deposit noble metal atoms and their oxides uniformly with a desirable thickness on the substrate by using sequential and self-limiting surface reaction^{47–51}. Generally, in this method, two precursors are used, and the deposition process involves four steps⁵²; (1) Initially, precursor is inserted in the chamber and allowed to react with the substrate; (2) Purging of reaction chamber by use of carrier gas; (3) Second precursor is inserted in the reaction chamber and allowed to react with substrate containing first precursor; (4) At last, purging of reaction chamber is done, and sample is obtained. By repeating the cycles, a desired thickness of the precursor can be deposited.

Sun et al.²⁷ synthesized heterogeneous catalysts consisting of isolated Pt atoms, Pt-clusters, Pt-nanoparticles dispersed on the surface graphene nanosheets (GNS) using ALD method, and also reported that these novel catalyst shows remarkable catalytic activity for methanol oxidation, almost ten times higher than the commercial carbon supported Pt (Pt/C) catalyst. For the synthesis of Pt/GNS catalyst (methylcyclopentadienyl)-trimethylplatinum (MeCpPtMe_3 , 98% purity) and oxygen (99.9995%) used as precursors and nitrogen (99.9995%) used as purge and carrier gas. The HAAD-STEM images of Pt/GNS catalyst synthesized with 50, 100, and 150 ALD cycles, reveals that isolated Pt atoms and small cluster (<1 nm) are present in the 50ALD-Pt/GNS (see Fig. 4 A), whereas in the 100ALD-Pt/GNS, and 150ALD-Pt/GNS the size cluster approaches to 2 nm and 4 nm, respectively. Recently, Cheng et al.⁵³ synthesized Pt/N-GNS SAC by same ALD technique discussed above, in which isolated Pt atoms are uniformly dispersed on the surface of nitrogen-doped graphene nano-sheets, and also investigated its activity for Hydrogen evolution reaction. They also reported, Pt/NGNs exhibits enhanced catalytic activity (≈ 37 times more than Pt/C) and high stability. The Pt loading of 2.1 and 7.6 wt% for 50 and 100 ALD cycles, respectively, was confirmed by inductively coupled plasma atomic emission spectroscopy. Similarly, as above, a bright spot of isolated Pt atoms, as well as tiny Pt cluster, are observed in 50ALD-

Pt/NGNs (see Fig. 4 B), whereas in 100ALD-Pt/NGNs, the size of Pt clusters becomes larger and formation of nanoparticles, as well as new cluster, is observed.

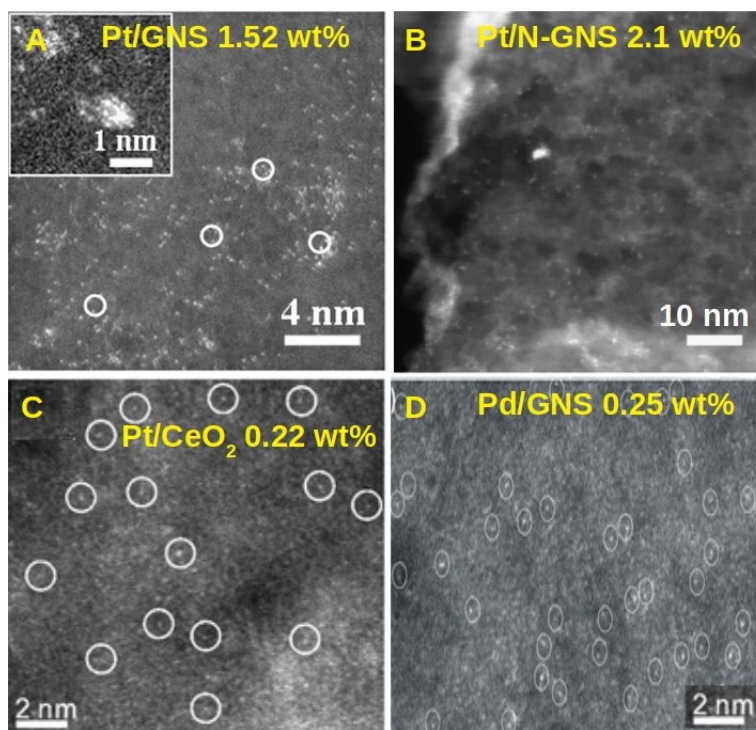


Figure 4: The figure represents the HAADF-STEM images of different single atom catalyst synthesized using atomic layer deposition method: (a) Pt/GNS, (b) Pt/N-GNS, (c) Pt_1/CeO_2 , (d) Pd/GNS. (a) reprinted/reproduce from Ref. [27] with the permission of Nature publishing group, copyright 2013, (b) reprinted/reproduce from Ref. [53] with the permission of Nature publishing group, copyright 2016, (c) reprinted/reproduce from Ref. [36] with the permission of American Chemical society publishing group, copyright 2016, (d) reprinted/reproduce from Ref. [28] with the permission of American Chemical society publishing group, copyright 2015.

Lu and co-workers²⁸ used ALD technique for preparation of single atom Pd_1 /graphene catalyst (see Fig. 4 D), palladium hexafluoroacetylacetate ($\text{Pd}(\text{hfac})_2$, Sigma Aldrich, 99%) and formalin (Aldrich, 37% HCHO and 15% CH_3OH in aqueous solution) used as precursors and N_2 (99.999%, purity) as carrier and purge gas. Researchers explored the hydrogenation of 1,3-butadiene using Pd_1 /graphene SAC and observed excellent durability for catalytic deactivation and remarkable catalytic performance, i.e., 100% butenes selectivity and 95% conversion at 50 °C. Wang et al.³⁶ from Lu group have synthesized single Pt_1/CeO_2 (see Fig. 4 C) catalyst and studied its activity in water promoted CO oxidation and reported that

the contribution of water in production CO₂ using Pt₁/CeO₂ is 50% via a water-mediated Mars-Van Krevelen (MvK) mechanism.

Piernavieja-Hermida et al.⁵⁴ developed an exciting way to stabilize single Pd atom on the surface of Al₂O₃ by depositing an ultra-thin layer of TiO₂ protective coatings. First, Pd(hfac)₂ precursor is allowed to chemisorb on the surface of Al₂O₃ using ALD; after that, TiO₂ is deposited on the substrate using tetrachloride and ionized water. The TiO₂ selectively grows on the substrate, not on the Pd(hfac)₂ because of the presence of remaining (hfac)₂, which prevents its growth on Pd. The massive structure of (hfac)₂ forms a nanocavity around the Pd atoms of same the dimension, and at last, these ligands are removed using formalin (HCHO) for obtaining the TiO₂ protected Pd/Al₂O₃ catalyst. They also reported that the thermal stability of this catalyst significantly increased because of the nanocavity thin-film structure. The HAADF-STEM images of single atoms catalysts Pt/GNS²⁷, Pt/N-GNS⁵³, Pt₁/CeO₂³⁶, and Pd/GNS²⁸ with 1.52 wt%, 2.1 wt%, 0.22 wt% and 0.25 wt%, respectively, are presented in Fig. 4.

The major disadvantages of the ALD technique are; it is a time-consuming method and ALD instruments and running cost are very expensive.

Metal-Organic Frameworks Derived Method

Metal-organic frameworks (MOFs)^{32,55,56} are the porous compound in which metal ions or clusters are attached with organic ligands to form 1-, 2- or 3- dimensional structure, and could be used as precursors or as support in the synthesis of SACs. Unique characteristics of MOFs such as high surface area, ordered pore structure with uniform sizes makes them ideal substrate for loading of single atom. In the synthesis of SACs, MOFs are emerging as a new research frontier because of the following reasons; (1) Tunable pore size enables MOFs to encapsulate metal precursors and prevent from the agglomeration. (2) The high surface area of MOFs provides a large number of anchoring sites for dispersion of metal precursors. (3) A variety of organic ligands serve as active anchoring sites for various precursors. (4) Using

the pyrolysis method, various MOFs can be easily converted into N-doped carbon materials, and act as a ideal substrate for dispersion and stabilization of metal precursors.

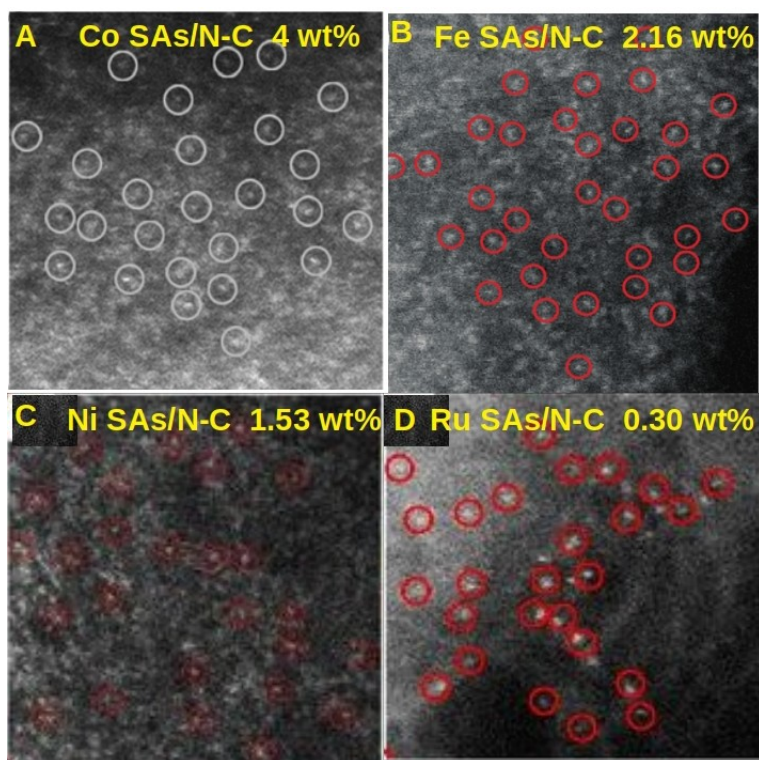


Figure 5: The figure represents the HAADF-STEM images of different single atom catalyst synthesized using metal-organic frameworks method: (a) Co SAs/N-C, (b) Fe SAs/N-C, (c) Ni SAs/N-C, (d) Ru SAs/N-C. (a) reprinted/reproduce from Ref. [29] with the permission of Wiley-VCH publishing group, copyright 2016, (b) reprinted/reproduce from Ref. [30] with the permission of Wiley-VCH publishing group, copyright 2017, (c) reprinted/reproduce from Ref. [31] with the permission of American Chemical society publishing group, copyright 2017, (d) reprinted/reproduce from Ref. [32] with the permission of American Chemical society publishing group, copyright 2017.

Yin et al.²⁹ from Li group synthesized single atom Co/N-C catalyst (see Fig. 5 A) with high metal loading up to 4 wt%, which consists Co atom dispersed on the surface of nitrogen-doped porous carbon and investigated its activity for oxygen reduction reaction. By performing the pyrolysis of bimetallic Zn/Co metal-organic framework (BMOF) at 800 °C, the Co and Zn ions are reduced by carbonization of organic ligands and further evaporation of Zn takes place because of its low boiling point and single atom Co/N-C catalyst is obtained. Wang et al.⁵⁷ from the same group reported that the coordination number of Co atom could

be controlled by changing the pyrolysis temperature, for example they fabricated three single atom Co-N₄, Co-N₃ and Co-N₂ catalyst by keeping the pyrolysis temperature at 800, 900 and 100 °C, respectively.

Chen *et al.*³⁰ also from Li group synthesized isolated Fe atom supported on nitrogen-doped porous carbon (Fe SAs/N-C) catalyst (see Fig. 5 B) with metal loading up to 2.16 wt% and reported its excellent activity for oxygen reduction reaction compared to Pt/C and most non-expensive-metal catalyst. They mixed Fe(acac)₃ and zeolitic imidazolate frameworks (ZIF-8) and used encapsulated-precursor pyrolysis technique for the synthesis of Fe/N-C catalyst. The molecular-scale cage structure of ZIF-8 formed by assembly of Zn²⁺ and 2-methylimidazole traps one Fe(acac)₃ molecule. After that, pyrolysis of resulting mixture at 900 °C under Ar gas converts ZIF-8 into nitrogen-doped porous carbon, and simultaneously Fe(acac)₃ was reduced by carbonized organic ligands, and Fe SAs/N-C catalyst is obtained.

Zhao *et al.*³¹ prepared isolated Ni atom dispersed on the nitrogen-doped porous carbon (Ni SAs/N-C) (see Fig. 5 C) with metal loading up to 1.53 wt% and investigated its activity for electroreduction of CO₂. The homogeneous aqueous solution of Ni(NO₃)₂ was mixed with a solution containing ZIF-8 powder dispersed in n-hexane and actively stirred for 3 hours so that salt completely absorbed, resulting sample was centrifuged and dried at 65 °C for 6 hours. After that, pyrolysis of the sample at 1000 °C was done in the presence of Ar gas, during which the ZIF-8 is converted into nitrogen-doped porous carbon, simultaneously Zn atoms evaporate due to its low boiling point, creating nitrogen-rich sites. These sites are occupied by Ni²⁺, and act as a fence and prevent Ni atom from agglomeration; finally, Ni SAs/N-C catalyst is obtained.

Wang *et al.*³² synthesized Ru SAs/N-C catalyst (see Fig. 5 D), which contains single Ru atom dispersed on the nitrogen-doped porous carbon with metal loading percentage 0.30 wt% and reported that it exhibits high catalytic and selectivity for hydrogenation of quinolines. They used amine derivative MOF UiO-66-NH₂ (Zr₆O₄(OH)₄(BDC)₆-NH₂) for synthesizing of Ru SAs/N-C catalyst, first, they mixed RuCl₃, ZrCl₄ and H₂BDC-NH₂ with an aqueous

solution of DMF and HAs. After that resulting mixture is centrifuged and washed with methanol and DMF and then heated at 700 °C for 3 hours in the presence of Ar gas, a black powder containing nitrogen-doped porous carbon (N-C) decorated with Ru and small ZrO_2 species is obtained. The small ZrO_2 species attach with N-C were etched by adding HF solution, and Ru SAs/N-C is formed.

Wei *et al.*⁵⁸ synthesized catalyst containing a single Pd atom supported on the nitrogen-doped porous carbon from Pd-nanoparticles by employing the top-down method, and also reported its excellent catalytic activity and selectivity for semi-hydrogenation of acetylene to ethylene. First, ZIF-8 nanocrystal was grown on the surface Pd-nanoparticles, by mixing Pd-nanoparticles in an aqueous solution $\text{Zn}(\text{NO}_3)_2$ and 2-methylimidazole solution. After that, the resulting mixture was heated at 900 °C in presences of inert gas for 3 hours, Pd-nanoparticles were transformed in single atoms and distributed within the substrate, and meanwhile, ZIF-8 is converted into nitrogen-doped porous carbon. Finally, single-atom Pd SAs/N-C is obtained having a thermodynamically stable Pd-N₄ structure. Using the same technique, they have also synthesized Pt SAs/N-C and Au SAs/N-C catalyst.

Using ZIF-8 MOF and pyrolysis method, Yang *et al.*⁵⁹ synthesized Ni SAs/N-C catalyst by transforming Ni nanoparticles into Ni single atom, mostly dispersed on the surface of N-doped porous carbon substrate and tested its activity and selectivity for electroreduction of CO_2 .

Recently, Zhang *et al.*⁶⁰ prepared Fe₁-N-C SAC using porphyrinic MOF (PCN-222), the catalyst contains isolated Fe atom dispersed on the surface of nitrogen-doped porous carbon substrate, and also reported its activity for nitrogen reduction reaction is better than Co₁-N-C and Ni₁-N-C. Initially, they synthesized Fe-TPPCOOMeCl (iron (III) meso-tetra(4-methoxycarbonylphenyl) porphine chloride (Fe-TPPCOOMeCl) by dissolving TPPCOOMe and $\text{FeCl}_2 \cdot 4\text{H}_2\text{O}$ in a DMF solution and heated for 6 hours at 160 °C. Then Fe-TCPP is obtained by mixing Fe-TPPCOOMeCl THF, MeOH and KOH, and heated for 6 hours at 85 °C. After that, Fe-TCPP, $\text{ZrOCl}_2 \cdot 8\text{H}_2\text{O}$, H_2 -TCPP, DMF and CF_3COOH were mixed

and heated for 18 hours at 120 °C for the formation of PCN-222(Fe). At last pyrolysis of PCN-222(Fe) sample is done at 800 °C for 3 hours in the presence of N₂ gas, and Fe₁-N-C catalyst is obtained. The HAADF-STEM images of single atoms catalysts Co SAs/N-C²⁹, Fe SAs/N-C³⁰, Ni SAs/N-C³¹, and Ru SAs/N-C³² with 4 wt%, 2.16 wt%, 1.53 wt% and 0.30 wt%, respectively, are presented in Fig. 5.

Application of Single-Atom Catalysis

In recent years, researchers have reported the synthesis and catalytic behavior of many SACs. They found that these SACs show high catalytic activity, selectivity, and stability because of the maximum utilization of single atom (almost 100% utilization) during reactions and strong bonding between the single atom and the anchoring sites on the supported surfaces. Therefore, the application of many SACs in different catalytic reactions such as CO oxidation, water-gas shift reaction, water splitting reaction, oxygen reduction reaction, methanol oxidation reaction, C-H activation reactions, Hydrogen evolution reaction, carbon dioxide reduction reaction and Hydrogenation reaction, are discussed below.

CO Oxidation Reaction

In the field of catalyst science, CO oxidation is one of the most studied reaction because of its importance in protecting our environment by purifying poisonous exhaust gases coming from motor vehicles and various Industries^{61,62}. Moreover, CO oxidation is the most crucial step in water-gas-shift reaction^{63,64} and in fuel cells application for eliminating CO from reforming gas. Zhang and co-workers¹⁶ were the first to investigate experimentally and theoretically the catalytic activity, selectivity and stability of single-atom Pt₁/FeO_x catalyst for CO oxidation, and relativistic density functional theory was used for theoretical investigation.

For computation, they used Fe- and O₃- terminated Fe₂O₃ (011) surfaces, and after optimization found that the most likeliest position of Pt atom is 3-fold hollow sites on the

O₃ terminated surface, where Pt atom is linked with three oxygen atom. From HAAD images, they observed that the single Pt atom exactly replaces the single Fe atom located at 3-fold hollow sites of O₃-terminated surface. Before testing the catalytic performance, the Pt₁/FeO_x catalyst was reduced by flowing H₂/He gas for 30 min at 200 °C. The oxidation of CO on the surface of Pt₁/FeO_x follows Langmuir-Hinshelwood (H-L) mechanism and the step by step reaction mechanism is shown in Fig. 6. After prereduction by H₂, the oxygen vacancy (O_{vac}) near the Pt atom was created by reducing the stoichiometric hematite surfaces partially (step i), which provides an active site for adsorption of O₂ molecule. A Similar theoretical model was designed for computation by removing one oxygen atom, which is connected to the Pt atom, the oxygen coordination number of Pt atom reduces from 3 to 2. In step ii, O₂ molecule is adsorbed with adsorption energy 1.05 eV, and optimize O-O bond length signifies that it is well activated by Pt atom and O_{vac}. Next, in step iii, CO molecule adsorbed on Pt₁ atom with binding energy 1.27 eV, and one of Oxygen atom of O₂ molecule comes nearer to CO molecule and form transition state (TS-1). The activation energy needed to process the reaction ($CO_{ad} + O - O_{ad} \rightarrow CO_2 + O_{ad}$) is 0.49 eV, and after releasing first CO₂ molecule from remaining O_{ad} atom restores the Pt-loaded stoichiometric hematite surface in step iv. In step v, another CO molecule adsorbed at Pt atom and migrated to an O_{ad} atom in step vi and form a second transition state (TS-2). The activation energy needed for the processing of the second reaction is 0.79 eV. After releasing the second CO₂ molecule, the Pt-loaded stoichiometric hematite surface reduced again to create new oxygen vacancy near Pt atom and approaches to initial step i. All of the catalytic steps are exothermic and the activation energy needed for formation of CO₂ molecule is small at low temperature, indicates that catalytic activity of Pt₁/FeO_x for CO oxidation is very high.

Liang *et al.* and Qiao *et al.* investigated experimentally as well as theoretically the catalytic activity of Ir₁/FeO_x³³, Au₁/FeO_x²² for CO oxidation, respectively.

Using DFT, Liang *et al.* explored the catalytic activity of non-noble metal single-atom catalyst (i.e., Ni₁/FeO_x³⁴) and also compared the catalytic activity of Pt₁/FeO_x, Ir₁/FeO_x

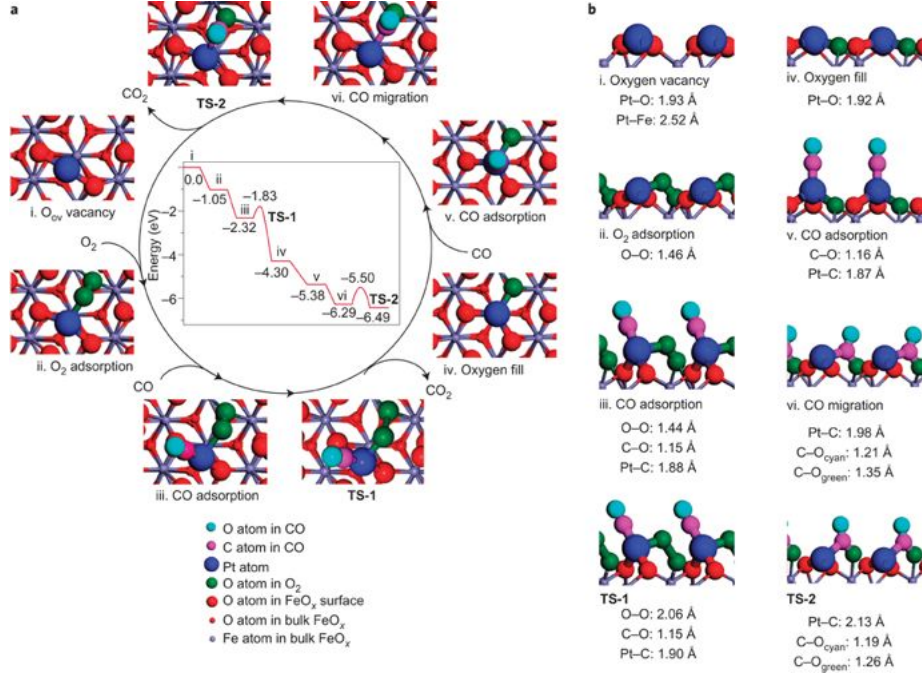


Figure 6: (a) Top and (b) side view of proposed reaction pathways for CO oxidation on Pt₁/FeO_x. The calculated relative energy of proposed reaction pathways is presented in circle. (reprinted/reproduce from Ref. [16] with the permission of Nature publishing group, copyright 2011).

and Ni₁/FeO_x systematically. The O₂ molecule adsorbed on the surface of these SACs in a different manner, in the case Pt₁/FeO_x and Ni₁/FeO_x it adsorbed on top of Pt and Ni atoms, respectively, whereas in the case and Ir₁/FeO_x it adsorbs dissociatively, i.e., one O atom on the top of Ir and another O atom occupy the oxygen vacancy site. The activation energy needed for the formation of CO₂ (TS-1) in the case of Pt₁/FeO_x, Ir₁/FeO_x and Ni₁/FeO_x catalysis is 0.49 eV, 0.59 eV and 0.75 eV, respectively, whereas for the formation of second CO₂ (TS-2) the activation barrier is 0.79 eV, 1.41 eV and 0.64 eV, respectively. The rate-determining step for Ni/FeO_x (0.75 eV) catalyst is lowest compared to Pt₁/FeO_x (0.79 eV) and Ir₁/FeO_x (1.41 eV) catalyst, suggest that it exhibits the highest catalytic activity for CO oxidation compared to others at room temperature.

Using experimental and theoretical methods, Moses-DeBusk *et al.*¹⁸ examine the catalytic activity of single Pt atom dispersed on an inert substrate, θ -Al₂O₃ for CO oxidation, in the presence of stoichiometric oxygen. They reported that the proposed pathway of CO oxidation

is slightly different from the conventional Langmuir-Hinshelwood mechanism because the conventional mechanism requires at least one Pt-Pt bond.

In search of non-precious and more efficient/active SACs for CO oxidation Li *et al.*³⁵ systematically studied the catalytic activity of various single-atom catalysts M_1/FeO_x ($M=Au, Rh, Pd, Co, Cu, Ru$ and Ti) by employing density functional theory. They reported five SACs, especially Rh_1/FeO_x and Pd_1/FeO_x with oxygen vacancy, Co_1/FeO_x and Ti_1/FeO_x without oxygen vacancy, and Ru_1/FeO_x with or without oxygen vacancy surface exhibits better catalytic activity compared to Pt_1/FeO_x . Furthermore, they also reported that non-precious single atom Co_1/FeO_x and Ti_1/FeO_x catalyst need very low activation energy for CO oxidation via L-H mechanism.

Using DFT calculation Tang *et al.*⁶⁵ systematically studied the catalytic activity of single Pt atom dispersed on the CeO_2 (111), (110) and (100) surfaces for CO oxidation via Mars-van Krevelen mechanism. They reported that the single Pt atom loaded on the ceria surfaces are thermodynamically stable, and the oxidation state of Pt atom on (111) and (100) surfaces is +4. In contrast, the oxidation state of (110) surface is +2 due to the spontaneous formation of O_2^{2-} species, which reduces the oxidation state of Pt atom from +4 to +2, making the $Pt_1@CeO_2$ (110) catalyst most stable.

Water-Gas Shift Reaction

The water-gas shift (WGS) reaction was discovered in 1780 by Italian physicist Felice Fontana, but its importance in the industrial sector was realized much later. In this reaction, carbon monoxide and water vapor reacts to form carbon dioxide and hydrogen molecule ($CO + H_2O \rightleftharpoons CO_2 + H_2$). WGS is a cost-effective and more efficient method for the production of hydrogen. In industrial sectors, a large amount of hydrogen is needed for various process such as ammonia synthesis via Haber-Bosch process, synthetic liquid fuels synthesis via Fischer-Tropsch method, hydro-treating of petroleum products for removing CO contamination, in the synthesis of nitrogenous fertilizers, for preparation of ethanol, methanol,

and dimethyl ether, and hydrogenation of hazardous wastes (PCBs and dioxins)^{66,67}.

Apart from this, from future aspects, hydrogen is considered to be one of the cleanest and renewable energy source because it can be stored and transported efficiently and after burning, it produces only water as a byproduct⁶⁸⁻⁷¹.

Due to the high catalytic activity, selectivity, and efficiency of SACs, many researchers have investigated its catalytic properties for WGS reaction^{19,37-41}. Fu *et al.*⁷² synthesized low-content (0.2 - 0.9 wt%) gold-cerium oxide catalyst and reported its activity and stability is high for WGS reaction. Yang *et al.* prepared SAC consisting of isolated Au atoms dispersed on titania support and reported that it exhibits excellent activity for WGS reaction at low temperatures. They stabilize Au atom on support by irradiating titania support by UV rays, which is suspended in ethanol solution, where the gold atom donates the separated electrons to $-OH$ groups. The Au atoms with surrounding extra surface $-OH$ groups act as active sites for the WGS reaction and also reported that its catalytic performance is better than Au/CeO₂^{72,73}. Flytzani-Stephanopoulos group members prepared single atom centric Pt (Pt(II)-O(OH)_x-) and Au (Au-O(OH)_x-) sites stabilize by sodium or potassium ion by making bond with it through $-O$ ligands on three different supports, and examine its catalytic activity for WGS reaction^{74,75}. They found that the reaction rate of Pt(II)-O(OH)_x- species for WGS reaction is same for all supports (i.e., anatase (TiO₂), a microporous K-type L-zeolite (KTLZ) and mesoporous silica MCM-41 ([Si]MCM41)) for Na-containing catalyst with 0.5 wt% Pt loading⁷⁴. Similar to finding of single-site Pt(II)-O(OH)_x- species, irrespective of the support KTLZ and [Si]MCM41, TiO₂, CeO₂, and Fe₂O₃ the reaction rate of Au-O(OH)_x- species is same with 0.25 wt%, 0.25 wt%, 0.12 wt%, 0.50 wt% and 1.16 wt% Au loading, respectively⁷⁵.

Lin *et al.*¹⁹ synthesized catalyst consisting of isolated Ir atom loaded on FeO_x support and found that it shows remarkable performance for WGS reaction. The catalytic activity of Ir₁/FeO_x is higher than its cluster and nano-particle counterparts, also higher than Au- or Pt-based catalyst⁷³. After extensive research, they found that the single atom is responsible

for $\approx 70\%$ catalytic activity in a single atom, clusters and nano-particles catalyst. The Ir atom helps FeO_x support in reduction for creating oxygen vacancy, which leads to enhance the catalytic activity of Ir_1/FeO_x .

In literature, it has been seen that the WGS reaction mainly follows three reaction mechanisms, i.e., redox, formate, and carboxyl mechanisms. Fu et al.⁷³ proposed that nano-structured gold-ceria oxide catalyst follows the redox mechanism for WGS reaction. In this reaction mechanism, CO atom adsorbed on Au atom and oxidized with the help of O atom of ceria oxide; after that, support is reoxidized by water, and hydrogen is released. Shido and Iwasawa^{76,77} were the first to propose the formate mechanism for WGS reaction, in this mechanism CO and H_2O molecule adsorbs on the surface of support, next CO molecule interact with surface OH group to form formate (HCOO) intermediate, which dissociate into CO_2 molecule and H atom, and finally, two H atom recombine to form H_2 molecule. Liu et al.⁷⁸, studied the catalytic activity Au clusters-ceria oxide ($\text{Au}_{4-6}/\text{CeO}_2$) catalyst for WGS reaction and found that it follows the carboxyl mechanism. In this mechanism, CO_{ad} adsorbs on Au, and H_2O dissociatively (H and OH) adsorbs on Au, the adsorbed CO_{ad} interact with OH_{ad} to form carboxyl (COOH) intermediate after that COOH dissociate into CO_2 molecule and H atom, and at last, two H atom recombine to form H_2 molecule. Song *et al.*⁴⁰ predicted the reaction mechanism of isolated and clustered Au atoms on $\text{CeO}_2(110)$ using density functional theory for WGS reaction.

Song *et al.*⁴⁰ by employing DFT methods studied reaction mechanism of isolated and clustered Au atoms on $\text{CeO}_2(110)$ surface for WGS activity, using both pathways redox and carboxyl mechanism. The carboxyl mechanism is more favorable than redox mechanism because it requires higher energy for breaking O–H bonds, which is directly involved in the production of H_2 and CO_2 .

Recently, Liang *et al.*⁴² studied the catalytic activity of Ir_1/FeO_x SAC for WGS reaction by using theoretical and experimental methods. In Fig. 7 (a) and (b), a schematic diagram of Ir_1/FeO_x with oxygen vacancy, and the surface lattice oxygen atom (red) around Ir

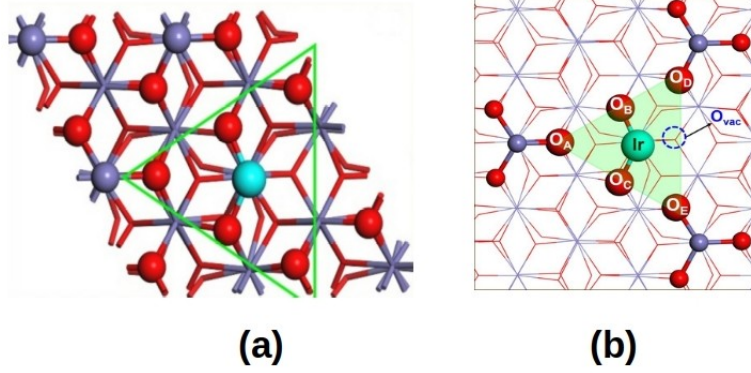


Figure 7: (a) The top view of SAC Ir₁/FeO_x with oxygen vacancy (O_{vac}) and (b) the local atomic arrangement of Ir₁/FeO_x–O_{vac} is shown in the figure. The surface lattice oxygen atom of FeO_x support are represented by O_A, O_B, O_C, O_D, O_E, and oxygen vacancy (O_{vac}) is situated at the right side of Ir atom. Ir atom= blue, Oxygen atom= red, and Fe atom= purple. (reprinted/reproduce from Ref. [42] with the permission of Wiley-VCH group, copyright 2020).

atom blue are represented, respectively. The most favorable position of Ir atom to stabilize on the surface of FeO_x is O₃–terminated surface, where Ir atom is bonded with three oxygen atom. The site structure of Ir₁/FeO_x with and without oxygen vacancy is the same, and it follows two different redox reaction pathways I and II, shown in Fig. 8 for WGS reaction.

Let us considered the reaction pathways I (Fig 8 (b)), in step (i) Ir atom is bonded with two oxygen, and on the right side of the Ir atom, there is an O_{vac}. Next, in step (ii) H₂O molecule dissociate into H and OH, and adsorbed on O_D atom (represented as H_a) and at O_{vac} site (represented as O_F for O atom and H_b for Hydrogen), respectively. The CO (O atom of CO is represented as O_G) molecule is absorbed on Ir₁ atom in step (iii). The next step is TS1, where H_a and H_b directly combine to form H₂ and require high activation energy 3.45 eV, which is also a rate-determining step. Afterwards the absorbed CO atom starts moving towards the O_F atom in step (iv) and gradually approaches to TS2. The energy barrier for the formation of CO₂ if the activation energy of 1 eV is applied. The newly form bent CO₂ molecule with a 140.7° angle still absorbs on Ir single atom in step (v). The bent CO₂ can be considered as a virtual CO[–]₂ anion, and its absorption energy on the Ir₁/FeO_x is 1.29 eV and require another intermediate step (vi) for relaxation. The bent CO[–]₂ transforms

into linear CO₂ by losing an electron in TS3, and the activation energy of TS3 is 0.59 eV. Finally, in step (vii), the desorption of CO₂ from the Ir₁/FeO_x and regeneration of O_{vac} occurs on the Ir atom's right side.

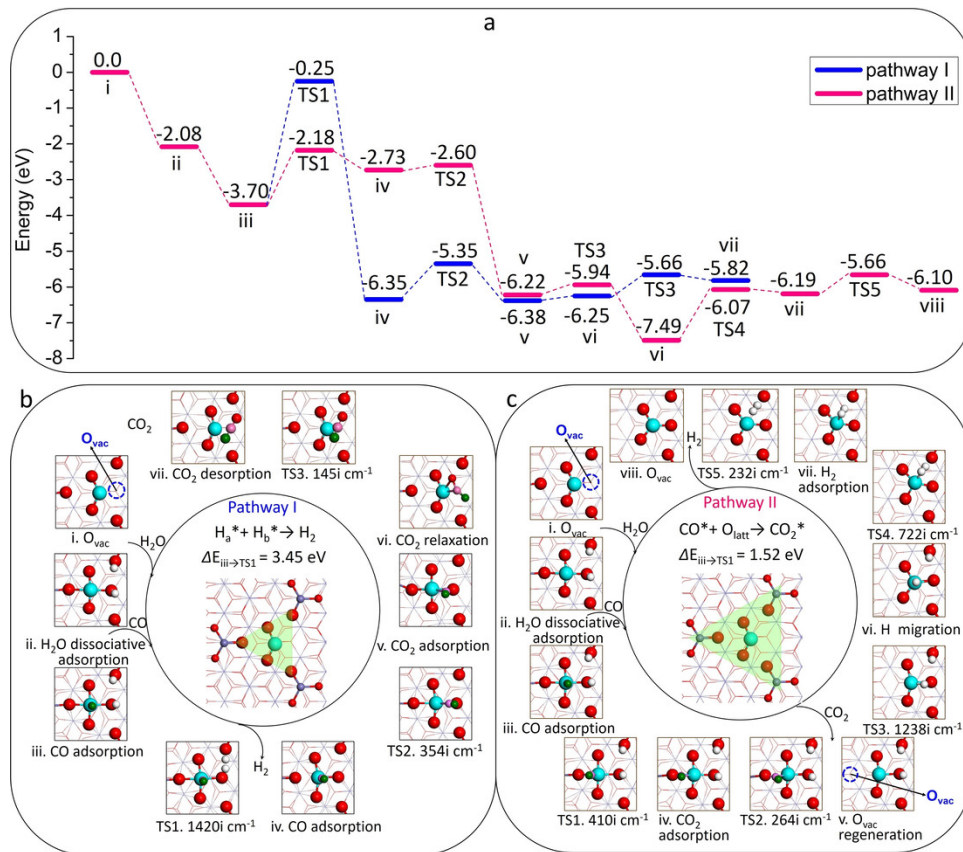


Figure 8: (a) The calculated relative energy diagram of proposed reaction pathways I and II for WGS reaction on Ir₁/FeO_x catalyst. The reaction step and corresponding structures for (b) path I and (c) path II are shown. The rate-determining step with the energy barrier is demonstrated in a circle, and a green triangle region represents active sites in the reaction. Ir atom= blue, Oxygen atom= red, Fe atom= purple, C atom = pink and O atom of CO= dark green. (reprinted/reproduce from Ref. [42] with the permission of Wiley-VCH group, copyright 2020).

The redox reaction pathways II is presented in Fig. 8 (c), and the reaction path till step (iii) is the same as pathways I. The Next step is TS1, which needs activation energy of 1.52 eV to move the adsorbed CO molecule slowly towards the adjacent O_a at the left side of Ir atom. The bent CO₂ (CO⁻₂) molecule is formed in step (iv). Afterward, the bent CO₂ requires small activation energy 0.13 eV for desorbing from the surface Ir₁/FeO_x by

releasing an electron in TS2. The O_{vac} on the left side of the Ir atom is produced after the desorption of CO_2 in step (v). The H_b atom of HO_F starts moving towards Ir atom slowly if small activation energy of 0.28 eV is applied in TS3. In the intermediate step (vi) H_a and H_b atoms are associated with O_D and Ir atom, respectively. The H_a and H_b approach towards each other in TS4 for the formation H_2 ($H_a^* + H_b^* \rightarrow H_2^*$), and energy barrier for the reaction is 1.42 eV. The obtained H_2 slowly migrate towards the Ir atom in step (vii). Next, H_2 molecule desorbs from the Ir_1/FeO_x in TS5 with an energy barrier of 0.53 eV. Finally, after releasing the H_2 molecule, the surface of Ir_1/FeO_x SAC is recovered, and O_{vac} is generated on the left side of Ir atom. During the WGS reaction process on Ir_1/FeO_x surface, O_{vac} shifts from the right side to the left side of Ir atom.

On comparing the pathways, we found that H_2 is first formed before CO_2 in pathways I, whereas in path II, it is reversed. The most favorable pathways for WGS reaction on Ir_1/FeO_x surface is path II, as the energy barrier for the rate-determining step is 1.52 eV, much lower compared to the Path I (3.45 eV). Using Bader charge analysis Liang *et al.*⁴² also reported the oxidation state of Ir and Fe atom for both pathways. In pathways I, only Ir atom changes its oxidation state, whereas, in pathways II, both Ir and Fe atom changes oxidation state. In step (i) of pathways II, the oxidation state of Ir and $Fe^{(a)}$ atom are +3 and +2, respectively, whereas in the final step (viii) the oxidation of Ir atom decreases from +3 to +2 and the oxidation state of Fe atom increases from +2 to +3. We can conclude that in WGS reaction Pathways II both Ir and Fe atom changes its oxidation state.

Summary and Conclusions

In this review article, we presented the recent advancement in the field of single-atom catalysis with a focus on the various synthesis methods and their application in various catalytic reactions, such as CO oxidation^{16,18,22,33–36}, water–gas shift (WGS)^{19,37–42}, etc. We also discussed the reaction mechanism of a single-atom catalyst for different catalytic reactions

from theoretical aspects using density functional theory.

Acknowledgements

D.K.R would like to thank Prof. Jun Li and Prof. Yang-Gang Wang for useful discussion and for giving the opportunity to write a review article on Single-Atom Catalysts. The author also gratefully acknowledges the financial support from the Southern University of Science and Technology (SUSTech) and computational resource support from the Center for Computational Science and Engineering at SUSTech.

References

- (1) Zhu, C.; Du, D.; Eychmuller, A.; Lin, Y. Engineering ordered and nonordered porous noble metal nanostructures: synthesis, assembly, and their applications in electrochemistry. *Chemical reviews* **2015**, *115*, 8896–8943.
- (2) Liu, X.; Iocozzia, J.; Wang, Y.; Cui, X.; Chen, Y.; Zhao, S.; Li, Z.; Lin, Z. Noble metal–metal oxide nanohybrids with tailored nanostructures for efficient solar energy conversion, photocatalysis and environmental remediation. *Energy & Environmental Science* **2017**, *10*, 402–434.
- (3) Cai, P.; Li, Y.; Wang, G.; Wen, Z. Alkaline–acid Zn–H₂O fuel cell for the simultaneous generation of hydrogen and electricity. *Angewandte Chemie* **2018**, *130*, 3974–3979.
- (4) Li, Z.; Liu, H.; Liu, Y.; He, P.; Li, J. A room-temperature ionic-liquid-templated proton-conducting gelatinous electrolyte. *The Journal of Physical Chemistry B* **2004**, *108*, 17512–17518.
- (5) Furstner, A. Gold and platinum catalysis a convenient tool for generating molecular complexity. *Chemical Society Reviews* **2009**, *38*, 3208–3221.

- (6) Zheng, N.; Zhang, T. Preface: single-atom catalysts as a new generation of heterogeneous catalysts. *National Science Review* **2018**, *5*, 625–625.
- (7) Zhang, S.; Nguyen, L.; Liang, J.-X.; Shan, J.; Liu, J.; Frenkel, A. I.; Patlolla, A.; Huang, W.; Li, J.; Tao, F. Catalysis on singly dispersed bimetallic sites. *Nature communications* **2015**, *6*, 1–10.
- (8) Herzing, A. A.; Kiely, C. J.; Carley, A. F.; Landon, P.; Hutchings, G. J. Identification of active gold nanoclusters on iron oxide supports for CO oxidation. *Science* **2008**, *321*, 1331–1335.
- (9) Turner, M.; Golovko, V. B.; Vaughan, O. P.; Abdulkin, P.; Berenguer-Murcia, A.; Tikhov, M. S.; Johnson, B. F.; Lambert, R. M. Selective oxidation with dioxygen by gold nanoparticle catalysts derived from 55-atom clusters. *Nature* **2008**, *454*, 981–983.
- (10) Liang, S.; Hao, C.; Shi, Y. The power of single-atom catalysis. *ChemCatChem* **2015**, *7*, 2559–2567.
- (11) Wang, A.; Li, J.; Zhang, T. Heterogeneous single-atom catalysis. *Nature Reviews Chemistry* **2018**, *2*, 65–81.
- (12) Yang, X.-F.; Wang, A.; Qiao, B.; Li, J.; Liu, J.; Zhang, T. Single-atom catalysts: a new frontier in heterogeneous catalysis. *Accounts of chemical research* **2013**, *46*, 1740–1748.
- (13) Liu, J. Catalysis by supported single metal atoms. *Acs Catalysis* **2017**, *7*, 34–59.
- (14) Cheng, N.; Zhang, L.; Doyle-Davis, K.; Sun, X. Single-atom catalysts: from design to application. *Electrochemical Energy Reviews* **2019**, 1–35.
- (15) Wang, Q.; Zhang, D.; Chen, Y.; Fu, W.-F.; Lv, X.-J. Single-atom catalysts for photocatalytic reactions. *ACS Sustainable Chemistry & Engineering* **2019**, *7*, 6430–6443.

- (16) Qiao, B.; Wang, A.; Yang, X.; Allard, L. F.; Jiang, Z.; Cui, Y.; Liu, J.; Li, J.; Zhang, T. Single-atom catalysis of CO oxidation using Pt₁/FeOx. *Nature Chemistry* **2011**, *3*, 634–641.
- (17) Kwon, Y.; Kim, T. Y.; Kwon, G.; Yi, J.; Lee, H. Selective activation of methane on single-atom catalyst of rhodium dispersed on zirconia for direct conversion. *Journal of the American Chemical Society* **2017**, *139*, 17694–17699.
- (18) Moses-DeBusk, M.; Yoon, M.; Allard, L. F.; Mullins, D. R.; Wu, Z.; Yang, X.; Veith, G.; Stocks, G. M.; Narula, C. K. CO oxidation on supported single Pt atoms: Experimental and ab initio density functional studies of CO interaction with Pt atom on θ -Al₂O₃ (010) surface. *Journal of the American Chemical Society* **2013**, *135*, 12634–12645.
- (19) Lin, J.; Wang, A.; Qiao, B.; Liu, X.; Yang, X.; Wang, X.; Liang, J.; Li, J.; Liu, J.; Zhang, T. Remarkable Performance of Ir₁/FeOx Single-Atom Catalyst in Water Gas Shift Reaction. *Journal of the American Chemical Society* **2013**, *135*, 15314–15317, PMID: 24090210.
- (20) Qiao, B.; Liu, J.; Wang, Y.-G.; Lin, Q.; Liu, X.; Wang, A.; Li, J.; Zhang, T.; Liu, J. J. Highly Efficient Catalysis of Preferential Oxidation of CO in H₂-Rich Stream by Gold Single-Atom Catalysts. *ACS Catalysis* **2015**, *5*, 6249–6254.
- (21) Qiao, B.; Lin, J.; Wang, A.; Chen, Y.; Zhang, T.; Liu, J. Highly active Au₁/Co₃O₄ single-atom catalyst for CO oxidation at room temperature. *Chinese Journal of Catalysis* **2015**, *36*, 1505 – 1511.
- (22) Qiao, B.; Liang, J.-X.; Wang, A.; Xu, C.-Q.; Li, J.; Zhang, T.; Liu, J. J. Ultrastable single-atom gold catalysts with strong covalent metal-support interaction (CMSI). *Nano Research* **2015**, *8*, 2913–2924.
- (23) Sun, X.; Lin, J.; Zhou, Y.; Li, L.; Su, Y.; Wang, X.; Zhang, T. FeOx supported single-

- atom Pd bifunctional catalyst for water gas shift reaction. *AIChE Journal* **2017**, *63*, 4022–4031.
- (24) Liu, P.; Zhao, Y.; Qin, R.; Mo, S.; Chen, G.; Gu, L.; Chevrier, D. M.; Zhang, P.; Guo, Q.; Zang, D. et al. Photochemical route for synthesizing atomically dispersed palladium catalysts. *Science* **2016**, *352*, 797–800.
- (25) Li, X.; Bi, W.; Zhang, L.; Tao, S.; Chu, W.; Zhang, Q.; Luo, Y.; Wu, C.; Xie, Y. Single-Atom Pt as Co-Catalyst for Enhanced Photocatalytic H₂ Evolution. *Advanced Materials* **2016**, *28*, 2427–2431.
- (26) Li, H.; Wang, L.; Dai, Y.; Pu, Z.; Lao, Z.; Chen, Y.; Wang, M.; Zheng, X.; Zhu, J.; Zhang, W. et al. Synergetic interaction between neighbouring platinum monomers in CO₂ hydrogenation. *Nature nanotechnology* **2018**, *13*, 411.
- (27) Sun, S.; Zhang, G.; Gauquelin, N.; Chen, N.; Zhou, J.; Yang, S.; Chen, W.; Meng, X.; Geng, D.; Banis, M. N. et al. Single-atom catalysis using Pt/graphene achieved through atomic layer deposition. *Scientific reports* **2013**, *3*, 1775.
- (28) Yan, H.; Cheng, H.; Yi, H.; Lin, Y.; Yao, T.; Wang, C.; Li, J.; Wei, S.; Lu, J. Single-atom Pd₁/graphene catalyst achieved by atomic layer deposition: remarkable performance in selective hydrogenation of 1, 3-butadiene. *Journal of the American chemical society* **2015**, *137*, 10484–10487.
- (29) Yin, P.; Yao, T.; Wu, Y.; Zheng, L.; Lin, Y.; Liu, W.; Ju, H.; Zhu, J.; Hong, X.; Deng, Z. et al. Single cobalt atoms with precise N-coordination as superior oxygen reduction reaction catalysts. *Angewandte chemie international edition* **2016**, *55*, 10800–10805.
- (30) Chen, Y.; Ji, S.; Wang, Y.; Dong, J.; Chen, W.; Li, Z.; Shen, R.; Zheng, L.; Zhuang, Z.; Wang, D. et al. Isolated single iron atoms anchored on N-doped porous carbon as an efficient electrocatalyst for the oxygen reduction reaction. *Angewandte Chemie International Edition* **2017**, *56*, 6937–6941.

- (31) Zhao, C.; Dai, X.; Yao, T.; Chen, W.; Wang, X.; Wang, J.; Yang, J.; Wei, S.; Wu, Y.; Li, Y. Ionic exchange of metal–organic frameworks to access single nickel sites for efficient electroreduction of CO₂. *Journal of the American Chemical Society* **2017**, *139*, 8078–8081.
- (32) Wang, X.; Chen, W.; Zhang, L.; Yao, T.; Liu, W.; Lin, Y.; Ju, H.; Dong, J.; Zheng, L.; Yan, W. et al. Uncoordinated amine groups of metal–organic frameworks to anchor single Ru sites as chemoselective catalysts toward the hydrogenation of quinoline. *Journal of the American Chemical Society* **2017**, *139*, 9419–9422.
- (33) Liang, J.-X.; Lin, J.; Yang, X.-F.; Wang, A.-Q.; Qiao, B.-T.; Liu, J.; Zhang, T.; Li, J. Theoretical and experimental investigations on single-atom catalysis: Ir₁/FeO_x for CO oxidation. *The Journal of Physical Chemistry C* **2014**, *118*, 21945–21951.
- (34) Liang, J.-X.; Yang, X.-F.; Wang, A.; Zhang, T.; Li, J. Theoretical investigations of non-noble metal single-atom catalysis: Ni₁/FeO_x for CO oxidation. *Catalysis Science & Technology* **2016**, *6*, 6886–6892.
- (35) Li, F.; Li, Y.; Zeng, X. C.; Chen, Z. Exploration of high-performance single-atom catalysts on support M₁/FeO_x for CO oxidation via computational study. *Acs Catalysis* **2014**, *5*, 544–552.
- (36) Wang, C.; Gu, X.-K.; Yan, H.; Lin, Y.; Li, J.; Liu, D.; Li, W.-X.; Lu, J. Water-mediated Mars–Van Krevelen mechanism for CO oxidation on ceria-supported single-atom Pt₁ catalyst. *Acs Catalysis* **2016**, *7*, 887–891.
- (37) Flytzani-Stephanopoulos, M.; Gates, B. C. Atomically dispersed supported metal catalysts. *Annual review of chemical and biomolecular engineering* **2012**, *3*, 545–574.
- (38) Thomas, J. M.; Saghi, Z.; Gai, P. L. Can a single atom serve as the active site in some heterogeneous catalysts? *Topics in Catalysis* **2011**, *54*, 588–594.

- (39) Flytzani-Stephanopoulos, M. Gold atoms stabilized on various supports catalyze the water–gas shift reaction. *Accounts of chemical research* **2013**, *47*, 783–792.
- (40) Song, W.; Hensen, E. J. Mechanistic aspects of the water–gas shift reaction on isolated and clustered Au atoms on CeO₂ (110): A density functional theory study. *Acs Catalysis* **2014**, *4*, 1885–1892.
- (41) Yang, M.; Allard, L. F.; Flytzani-Stephanopoulos, M. Atomically dispersed Au–(OH) *x* species bound on titania catalyze the low-temperature water-gas shift reaction. *Journal of the American Chemical Society* **2013**, *135*, 3768–3771.
- (42) Liang, J.-X.; Lin, J.; Liu, J.; Wang, X.; Zhang, T.; Li, J. Dual Metal Active Sites in an Ir₁/FeO_x Single-Atom Catalyst: A Redox Mechanism for the Water-Gas Shift Reaction. *Angewandte Chemie International Edition* **2020**,
- (43) Yang, S.; Kim, J.; Tak, Y. J.; Soon, A.; Lee, H. Single-Atom Catalyst of Platinum Supported on Titanium Nitride for Selective Electrochemical Reactions. *Angewandte Chemie International Edition* **2016**, *55*, 2058–2062.
- (44) Choi, C. H.; Kim, M.; Kwon, H. C.; Cho, S. J.; Yun, S.; Kim, H.-T.; Mayrhofer, K. J.; Kim, H.; Choi, M. Tuning selectivity of electrochemical reactions by atomically dispersed platinum catalyst. *Nature communications* **2016**, *7*, 10922.
- (45) Lin, J.; Qiao, B.; Li, N.; Li, L.; Sun, X.; Liu, J.; Wang, X.; Zhang, T. Little do more: a highly effective Pt₁/FeO_x single-atom catalyst for the reduction of NO by H₂. *Chem. Commun.* **2015**, *51*, 7911–7914.
- (46) Xing, J.; Chen, J. F.; Li, Y. H.; Yuan, W. T.; Zhou, Y.; Zheng, L. R.; Wang, H. F.; Hu, P.; Wang, Y.; Zhao, H. J. et al. Stable isolated metal atoms as active sites for photocatalytic hydrogen evolution. *Chemistry–A European Journal* **2014**, *20*, 2138–2144.

- (47) Cheng, N.; Sun, X. Single atom catalyst by atomic layer deposition technique. *Chinese Journal of Catalysis* **2017**, *38*, 1508–1514.
- (48) George, S. M. Atomic layer deposition: an overview. *Chemical reviews* **2009**, *110*, 111–131.
- (49) O'Neill, B. J.; Jackson, D. H.; Lee, J.; Canlas, C.; Stair, P. C.; Marshall, C. L.; Elam, J. W.; Kuech, T. F.; Dumesic, J. A.; Huber, G. W. Catalyst design with atomic layer deposition. *Acs Catalysis* **2015**, *5*, 1804–1825.
- (50) Lu, J.; Elam, J. W.; Stair, P. C. Synthesis and stabilization of supported metal catalysts by atomic layer deposition. *Accounts of chemical research* **2013**, *46*, 1806–1815.
- (51) Liu, J.; Sun, X. Elegant design of electrode and electrode/electrolyte interface in lithium-ion batteries by atomic layer deposition. *Nanotechnology* **2014**, *26*, 024001.
- (52) Cheng, N.; Shao, Y.; Liu, J.; Sun, X. Electrocatalysts by atomic layer deposition for fuel cell applications. *Nano Energy* **2016**, *29*, 220–242.
- (53) Cheng, N.; Stambula, S.; Wang, D.; Banis, M. N.; Liu, J.; Riese, A.; Xiao, B.; Li, R.; Sham, T.-K.; Liu, L.-M. et al. Platinum single-atom and cluster catalysis of the hydrogen evolution reaction. *Nature communications* **2016**, *7*, 13638.
- (54) Piernavieja-Hermida, M.; Lu, Z.; White, A.; Low, K.-B.; Wu, T.; Elam, J. W.; Wu, Z.; Lei, Y. Towards ALD thin film stabilized single-atom Pd catalysts. *Nanoscale* **2016**, *8*, 15348–15356.
- (55) Zhang, H.; Wei, J.; Dong, J.; Liu, G.; Shi, L.; An, P.; Zhao, G.; Kong, J.; Wang, X.; Meng, X. et al. Efficient Visible-Light-Driven Carbon Dioxide Reduction by a Single-Atom Implanted Metal–Organic Framework. *Angewandte Chemie International Edition* **2016**, *55*, 14310–14314.

- (56) He, T.; Chen, S.; Ni, B.; Gong, Y.; Wu, Z.; Song, L.; Gu, L.; Hu, W.; Wang, X. Zirconium–porphyrin-based metal–organic framework hollow nanotubes for immobilization of noble-metal single atoms. *Angewandte Chemie International Edition* **2018**, *57*, 3493–3498.
- (57) Wang, X.; Chen, Z.; Zhao, X.; Yao, T.; Chen, W.; You, R.; Zhao, C.; Wu, G.; Wang, J.; Huang, W. et al. Regulation of coordination number over single Co sites: triggering the efficient electroreduction of CO₂. *Angewandte Chemie International Edition* **2018**, *57*, 1944–1948.
- (58) Wei, S.; Li, A.; Liu, J.-C.; Li, Z.; Chen, W.; Gong, Y.; Zhang, Q.; Cheong, W.-C.; Wang, Y.; Zheng, L. et al. Direct observation of noble metal nanoparticles transforming to thermally stable single atoms. *Nature nanotechnology* **2018**, *13*, 856.
- (59) Yang, J.; Qiu, Z.; Zhao, C.; Wei, W.; Chen, W.; Li, Z.; Qu, Y.; Dong, J.; Luo, J.; Li, Z. et al. In Situ Thermal Atomization To Convert Supported Nickel Nanoparticles into Surface-Bound Nickel Single-Atom Catalysts. *Angewandte Chemie International Edition* **2018**, *57*, 14095–14100.
- (60) Zhang, R.; Jiao, L.; Yang, W.; Wan, G.; Jiang, H.-L. Single-atom catalysts templated by metal–organic frameworks for electrochemical nitrogen reduction. *Journal of Materials Chemistry A* **2019**, *7*, 26371–26377.
- (61) Gardner, S. D.; Hoflund, G. B.; Upchurch, B. T.; Schryer, D. R.; Kielin, E. J.; Schryer, J. Comparison of the performance characteristics of Pt/SnO_x and Au/MnO_x catalysts for low-temperature CO oxidation. *Journal of Catalysis* **1991**, *129*, 114–120.
- (62) Haruta, M. Size-and support-dependency in the catalysis of gold. *Catalysis today* **1997**, *36*, 153–166.
- (63) Gokhale, A. A.; Dumesic, J. A.; Mavrikakis, M. On the mechanism of low-temperature

- water gas shift reaction on copper. *Journal of the American Chemical Society* **2008**, *130*, 1402–1414.
- (64) Lin, J.; Wang, A.; Qiao, B.; Liu, X.; Yang, X.; Wang, X.; Liang, J.; Li, J.; Liu, J.; Zhang, T. Remarkable performance of Ir1/FeO x single-atom catalyst in water gas shift reaction. *Journal of the American Chemical Society* **2013**, *135*, 15314–15317.
- (65) Tang, Y.; Wang, Y.-G.; Li, J. Theoretical investigations of Pt1@ CeO2 single-atom catalyst for CO oxidation. *The Journal of Physical Chemistry C* **2017**, *121*, 11281–11289.
- (66) Ramachandran, R.; Menon, R. K. An overview of industrial uses of hydrogen. *International Journal of Hydrogen Energy* **1998**, *23*, 593–598.
- (67) Ratnasamy, C.; Wagner, J. P. Water Gas Shift Catalysis. *Catalysis Reviews* **2009**, *51*, 325–440.
- (68) Chen, X.; Shen, S.; Guo, L.; Mao, S. S. Semiconductor-based photocatalytic hydrogen generation. *Chemical reviews* **2010**, *110*, 6503–6570.
- (69) LeValley, T. L.; Richard, A. R.; Fan, M. The progress in water gas shift and steam reforming hydrogen production technologies—a review. *international journal of hydrogen energy* **2014**, *39*, 16983–17000.
- (70) Pagliaro, M.; Konstandopoulos, A. G.; Ciriminna, R.; Palmisano, G. Solar hydrogen: fuel of the near future. *Energy & Environmental Science* **2010**, *3*, 279–287.
- (71) Turner, J. A. Sustainable Hydrogen Production. *Science* **2004**, *305*, 972–974.
- (72) Fu, Q.; Deng, W.; Saltsburg, H.; Flytzani-Stephanopoulos, M. Activity and stability of low-content gold–cerium oxide catalysts for the water–gas shift reaction. *Applied Catalysis B: Environmental* **2005**, *56*, 57–68.

- (73) Fu, Q.; Saltsburg, H.; Flytzani-Stephanopoulos, M. Active nonmetallic Au and Pt species on ceria-based water-gas shift catalysts. *Science* **2003**, *301*, 935–938.
- (74) Yang, M.; Liu, J.; Lee, S.; Zugic, B.; Huang, J.; Allard, L. F.; Flytzani-Stephanopoulos, M. A common single-site Pt (II)–O (OH) x-species stabilized by sodium on active and inert supports catalyzes the water-gas shift reaction. *Journal of the American Chemical Society* **2015**, *137*, 3470–3473.
- (75) Yang, M.; Li, S.; Wang, Y.; Herron, J. A.; Xu, Y.; Allard, L. F.; Lee, S.; Huang, J.; Mavrikakis, M.; Flytzani-Stephanopoulos, M. Catalytically active Au–O (OH) x-species stabilized by alkali ions on zeolites and mesoporous oxides. *Science* **2014**, *346*, 1498–1501.
- (76) Shido, T.; Iwasawa, Y. Regulation of reaction intermediate by reactant in the water-gas shift reaction on CeO₂, in relation to reactant-promoted mechanism. *Journal of Catalysis* **1992**, *136*, 493 – 503.
- (77) Shido, T.; Iwasawa, Y. Reactant-Promoted Reaction Mechanism for Water-Gas Shift Reaction on Rh-Doped CeO₂. *Journal of Catalysis* **1993**, *141*, 71 – 81.
- (78) Liu, Z.-P.; Jenkins, S. J.; King, D. A. Origin and Activity of Oxidized Gold in Water-Gas-Shift Catalysis. *Phys. Rev. Lett.* **2005**, *94*, 196102.